Rhenium(II) Complexes as Potential materials for Dye Sensitized Solar Cells

THESIS

Presented in Partial Fulfillment of the Requirements for the Degree Master of Science in the Graduate School of The Ohio State University

By

Ivan M. Cussianovich

Graduate Program in Chemistry

The Ohio State University

2013

Master's Examination Committee:

Dr. Claudia Turro, Advisor

Dr. Yiying Wu

Abstract

Tandem dye sensitized solar cells, in which both the anode and cathode are photo sensitive, had been proved to improve the overall efficiency of a DSSC. The compounds $[Re(dppe)_2Cl_2]Cl$ and $[Re(dppe)_2O_2]ClO_4$, where dppe is 1,2-bis(diphenylphosphino)ethane, were synthesized as potential materials for the photo cathode in a dye sensitized solar cell. Both compounds are synthesized from the same precursor, $[(Bu)_4N]_2[Re_2Cl_8]$, which is sintesized from $NaReO_4$. The compounds were characterized by ^1H NMR and ESI-MS.

Spectrophotometric measurements were performed for both complexed, founding that both exhibit appreciable emission around 600 nm. A cyclic voltammogram was obtained for the $[Re(dppe)_2Cl_2]Cl$ complex, and it was determined that the first reduction of this compound is reversible. The preliminary data suggests that the $[Re(ddppe)_2Cl_2]Cl$ compound may be suitable as a dye for the photo cathode in a tandem DSSC.

Dedication

This thesis is dedicated to my family.

Acknowledgments

I would like to thank my advisor Dr. Claudia Turro for her guidance and enthusiasm towards this research. I also want to thank the Turro group for always being there and lending a hand whenever help was needed.

Vita

December 2001 .....Santa María Marianistas High School

July 2008.....B.S. Chemistry, Universidad Nacional de Ingeniería

July 2010.....M.S. Chemistry, University of North Carolina at Charlotte

2010 to present .....Graduate Teaching Associate, Department of Chemistry, The Ohio State University

Fields of Study

Major Field: Chemistry

Table of Contents

List of Figures

Chapter 1: Introduction

1.1. Solar Cells

A solar cell is a device that converts light into electricity by means of the photoelectric effect. The processes involved are, the absorption of a photon from the sunlight by a semiconductor material or dye molecule, electron injection from the dye to the semiconductor and the regeneration of the dye by a redox couple.[1] As a result, solar energy is converted into electricity. There is a wide range of applications for these devices, which go from small cells to power calculators and toys, all the way up to powering satellites and the international space station.

Chapin *et. al* working at Bell Telephone Laboratories in 1954 developed a crystlline silicon solar cell with an efficiency of 6%, which represents the first example of a practical conversion of solar radiation into electricity.[2] The common solar power conversion efficiencies of modern solar cells are between 15 and 20%.[3] However, there are two main disadvantages with these types of solar cells. The first is the relatively high cost of manufacturing these cells, and the second is that toxic chemicals are involved in

manufacturing process.[3] These aspects prompted the search for environmentally friendly and low cost solar cells alternatives.

1.2 Dye-Sensitized Solar Cells (DSSC)

In 1991, Grätzel *et. al*[4] developed a new type of solar cell, now known as the dye-sensitized nanocrystalline solar cell, or Grätzel cell, which represents a good alternative to the standard silicon cell. The efficiency reported for the Grätzel cell was 7.1-7.9%, however the highest efficiency achieved today is 12.3%.[5] The key difference between the semiconductor, or conventional solar cell described in section 1.1 and the DSSC, is that the light absorption and charge transfer, both of which take place at the semiconductor in the former are two separate processes in the latter. This attribute makes the use of low- to medium- purity materials possible for this type of solar cells, lowering the price of the materials needed, while providing a commercially realistic conversation efficiency.[6] Moreover, the materials used in the production are environmental friendly.

A diagram of a conventional DSSC cell is shown in Figure 1, which consists of two conducting glass sheets as the electrodes coated with a transparent conductive layer, typically indium tin oxide. The working electrode is coated with titanium dioxide nanoparticles which have the dye adsorbed onto their surface, whereas the counter electrode, is coated with platinum or graphite. Between the two electrodes, there is is an electrolyte solution that contains the redox couple that regenerates the dye.

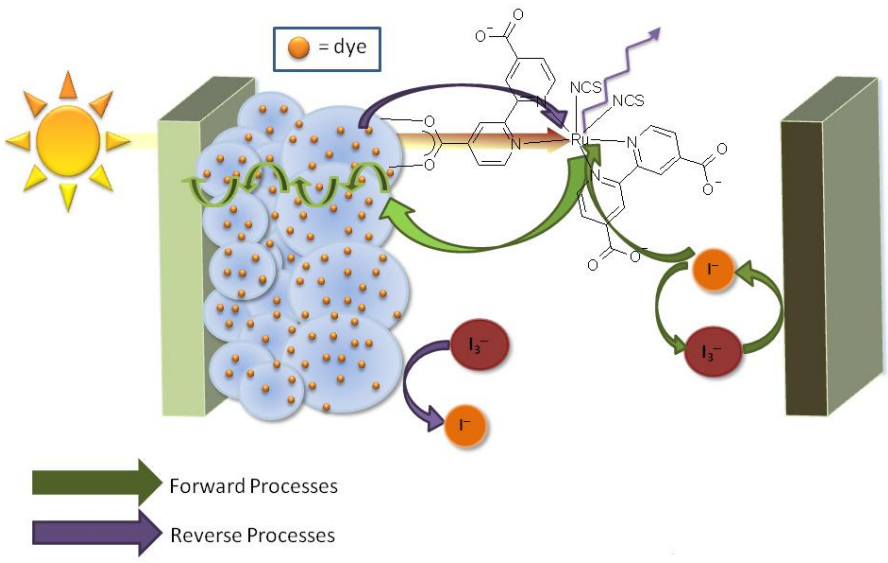

Figure 1: Dye-sensitized solar cell diagram

A scheme showing the operating principles of a DSSC is shown in Figure 2. The process begins when incident light is absorbed by the dye, placing it in an excited state that is able to inject an electron into the conduction band of the titanium dioxide semiconductor. Electron injection is followed by the movement of the electrons around the circuit to perform work, while the dye in solution remains oxidized. The dye is then restored by electron donation from the iodide/triiodide redox couple in solution, which is the most commonly used relay. Finally the iodide is regenerated by the reduction of triiodide at the counter electrode.

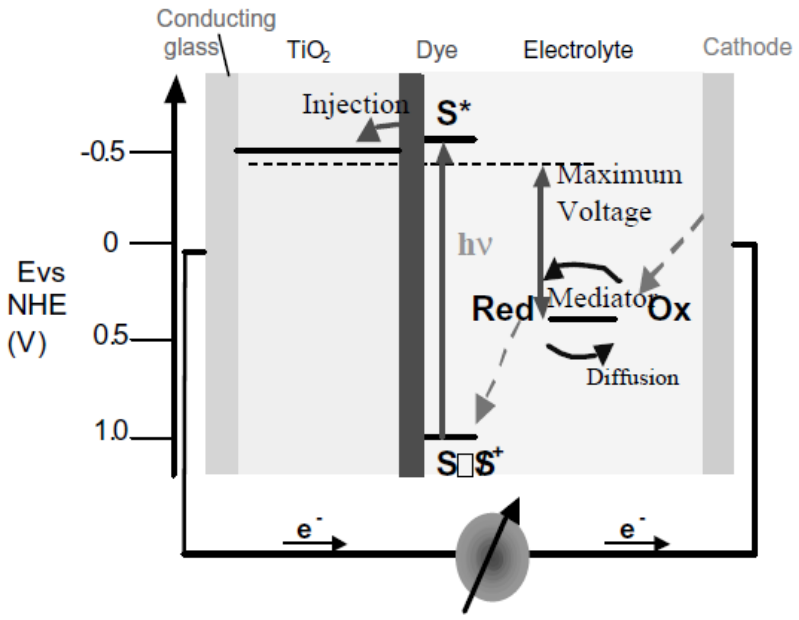

Figure 2: Principles of Operation of a DSSC

An important factor in the overall efficiency of DSCCs is the dye, since it represents the key component of the system. Therefore, analyzing the efficiency of the dye is extremely important. The dye efficiency can be determined by calculating how many absorbed photons give rise to electron injection and how many of those electrons are collected to generate electricity, given by the the incident photon to current efficiency (IPCE). The IPCE is expressed in the eq 1 and measures the amount of photons that give rise to the electric current.[7]

$$IPCE(\lambda) = LHE(\lambda) \times \Phi(inj) \times \eta(c) \quad (1)$$

Where LHE(λ) is the light harvesting energy given by the percentage of photons absorbed at a particular wavelength, Φ(inj) is the electron injection efficiency which

determines how many absorbed photons result in injected electrons to the semi-conductor, and $\eta(c)$ is the charge collection efficiency the fraction of the injected electrons are collected for electrical use.

It is important to note that all the processes involved in a DSSC cell are kinetic and therefore, their efficiency is determined by how fast they occur relative to other processes.

There are certain characteristics that a dye in a DSSC cell must possess to be considered successful. These include adsorption of the dye into the titanium dioxide, the effectively absorption of light, efficiently injection of the electrons, energy levels that match the conduction band of the semi-conductor, facile regeneration by the redox couple and stability for millions of cycles.[1]

Adsorption of the dye onto the titanium dioxide surface can be facilitated through the attachment of a substituent that binds to the surface. One of the most investigated dyes is the ruthenium based N3 dye shown in Figure 3. It can be seen that the carboxylic acid groups help the dye bind to the surface of the titanium dioxide. The absorption of visible light by the dye results in a metal-to-ligand charge transfer (MLCT), involving an electron transfer from the metal d-orbitals to the unoccupied π^* orbital of the carboxylated bipyridyl ligand.

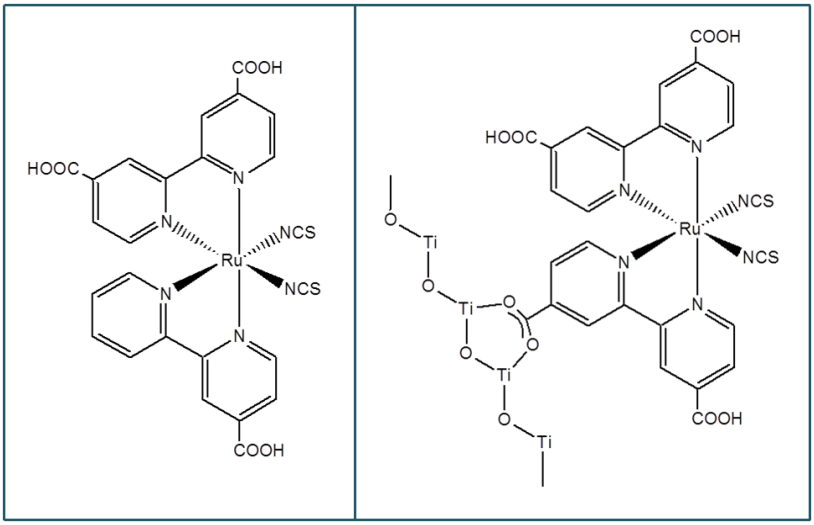

Figure 3: Ruthenium based N3 dye (left) and dye adsorbed onto TiO2 surface (right)

An important role of the dye is the absorption of light, therefore, the dye should absorb strongly from the blue end of the visible spectrum to the near infrared. Even though the ruthenium based N3 dye is the best dye available now, it possesses two mayor limitations. The first is the relatively low extinction coefficient (ε = 1-2 x 10^4 $M^{-1}cm^{-1}$), therefore, the development of dyes with greater extinction coefficients is a useful strategy. Several organic dyes have been tried out and their structures are shown in Figure 4.[7] These dyes have a larger extinction coefficient (ε = 5-20 x 10^5), but they absorb in a narrow range.

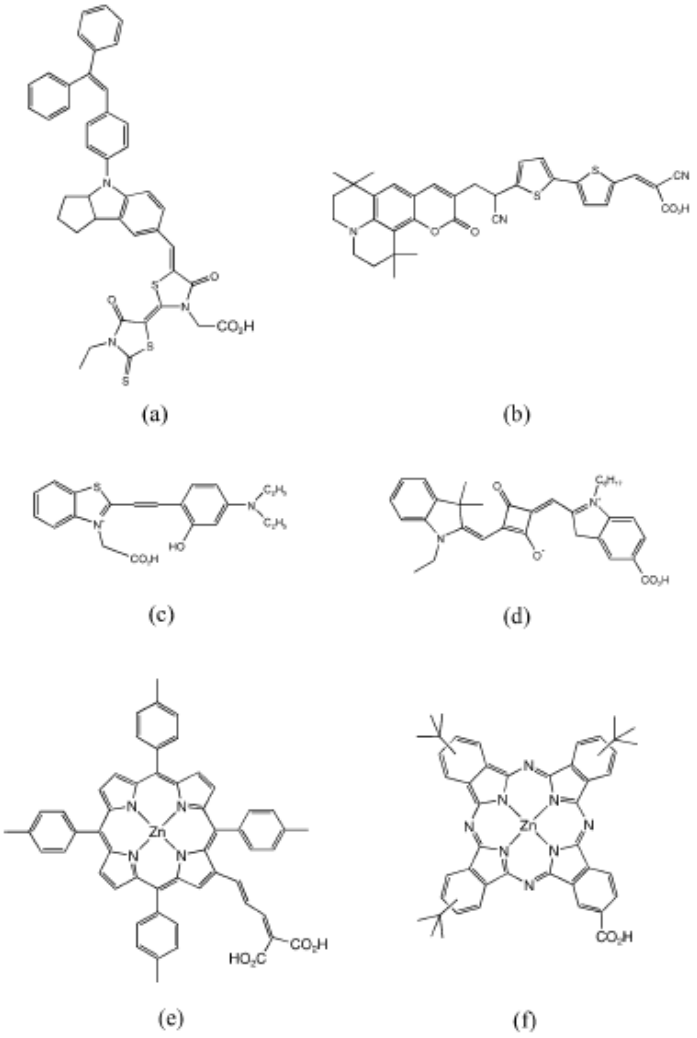

Figure 4: Some organic dyes tested for use in DSSCs

The other mayor limitation is that, as seen in Figure 5, the ruthenium based N3 dye does not absorb in the 750-900 nm region of the spectrum.[7] The overlap with the solar spectrum can be increased by shifting the absorption of the dye to lower energies, as shown in Figure 5.

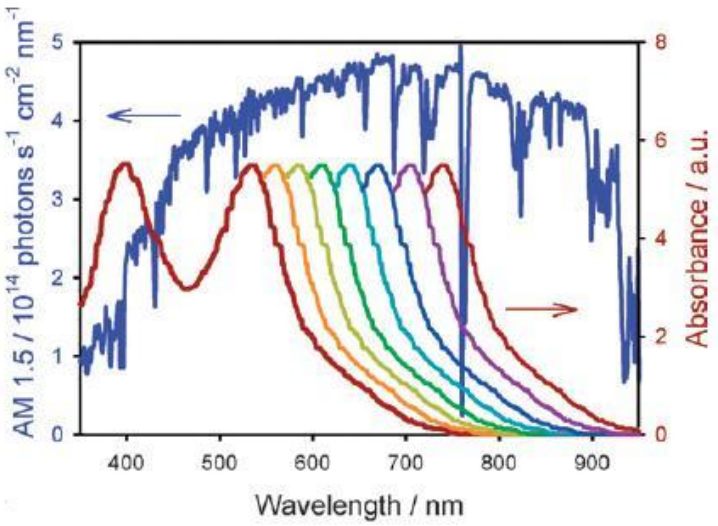

Figure 5: Solar spectrum and Ru-N3 dye (left-most red spectrum) / additional spectra changing energy gap

For the electron transfer from the excited dye to TiO_2 to be favorable, the excited state of the dye has to be higher in energy than the conduction band of the semiconductor. Additionally, the kinetics of the electron injection into the semiconductor has to be faster than the recombination of the dye. As shown in Figure 6, the N3 dye doesn't present any problems with respect to electron injection, because the electron injection is very fast and charge injection take place from both the ^{1}MLCT and the ^{3}MLCT states. Since the decay of the ^{1}MLCT is known to be in the femtosecond to picosecond timescales, the charge injection from the singlet state must be faster than the decay.[7]

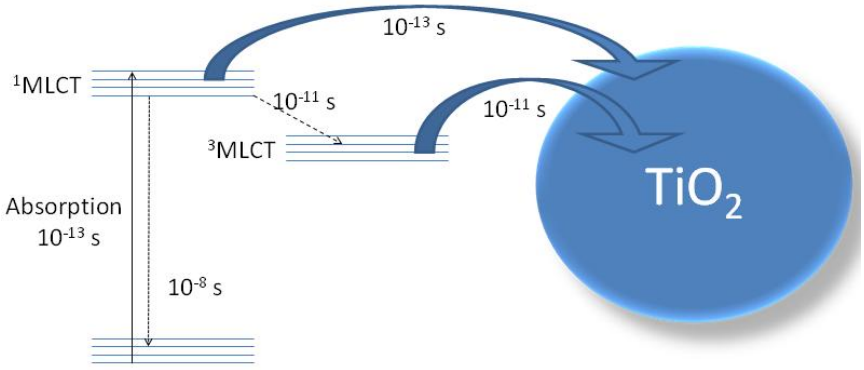

Figure 6: Timescales for the N3 dye

After the electron injection into the metal oxide, the next step is for the electrons to pass through the oxide layer onto the working electrode. TiO_2 is the substrate that is most commonly used, because it is inert, inexpensive and absorbs very little of the solar spectrum. One of Grätzel's innovations was the use of nanocrystalline TiO_2, which has significantly greater surface area, making it possible to adsorb more molecules of the dye molecules onto the surface. However, an important disadvantage is the slow time that the electrons take to pass through the metal oxide onto the electrode. As a result of this, trying to improve the electron diffusion through the oxide is an ongoing important area of research. One strategy is to use nanotubes or nanorods instead of nanoparticles, which provide a pathway for the electrons from the particle to the electrode, but possess a smaller surface area.[8]

The final component to be analyzed in a DSSC is the electrolyte containing the redox couple which regenerates the dye. The redox couple has to be efficient at reducing the dye back to the original state so another cycle can take place, but not capture or

intercept any of the electrons injected into the semiconductor. The latter involves an electron transfer from the conduction band of TiO_2 to the redox couple, lowering the efficiency of the overall process. The most efficient redox couple used to date is the iodide/triiodide and is the most commonly used. Improving the redox couple is difficult because the chemistry involved is not well understood,[9] but one appealing approach is the use of solid state redox couples, which provides greater concentrations of the redox couple, and are thus expected to improve efficiency.[7]

1.3 Tandem Dye-Sensitized Solar Cells

As described in the previous section, a dye sensitized solar cell consists of a photoactive anode and a passive cathode, where the purpose of the latter is only to regenerate the redox couple. In 2000, He *et al.*[10] reported the first tandem dye-sensitized solar cell which consisted on a nickel oxide, NiO, cathode and a TiO_2 anode, where both were dye-sensitized photoactive electrodes. This concept was developed as an attempt to improve the efficiency of a DSSC. The theoretical upper limit for a cell with only one photoactive electrode is ~30%, while for a device with two photoactive electrodes is 43%.[10]

A scheme of a tandem dye-sensitized solar cell is shown in Figure 7.[11] Light is absorbed by both dyes in separate processes, which gives rise to an electron to be injected into the conduction band of the TiO_2 anode and, at the same time, a hole to be injected

into the NiO cathode. These processes are followed by the diffusion of the charges through the respective semiconductors to the charge collectors. Finally the oxidized and reduced forms of the redox couple regenerate the dye cathode and anode, a process that is mediated by a Co(II/III) redox mediator in solution (Figure 7).

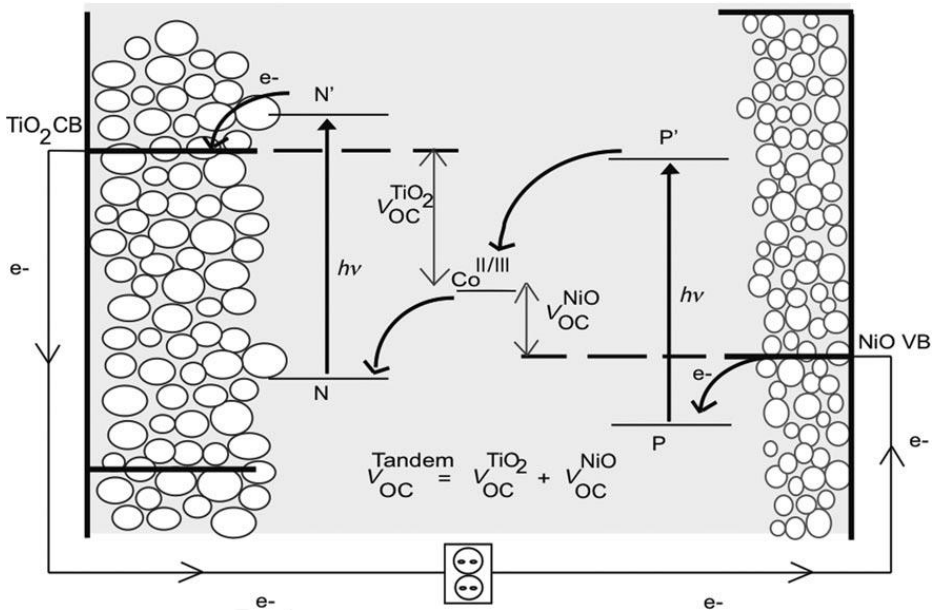

Figure 7: Scheme of a tandem dye-sensitized solar cell

It is important to note that for a device such as that shown in Figure 7 to work, the position of the energy levels of the dyes and semiconductors must be carefully selected. The HOMO (highest occupied molecular orbital) of the dye at the photocathode has to be below the valence band of NiO, and the LUMO (lowest unoccupied molecular orbital) of the same dye has to be above the energy level of the redox couple. Every single process

that takes place must be thermodynamically favorable in order to increase the efficiency of the cell.[11]

1.4 Research Goals

In 2006, Del Negro *et al.* reported highly oxidizing excited states for a rhenium complex.[12] The $[Re(dmpe)_3]^{2+}$ complex, (dmpe = 1,2-bis(dimethylphosphino)ethane), has an excited-state reduction potential of +2.58V. Taking this into consideration, the goals of this project is the synthesis of a series of compounds related to $[Re(dmpe)_3]^{2+}$, expecting that they will possess similar properties, but with the ability to be chemically modified such that they can be coupled to a semiconductor. The complexes chosen are $[Re(dppe)_3]^{2+}$, (dppe = 1,2-bis(diphenylphosphino)ethane; Figure 8), $[Re(dppe)_2(py)_2]^{2+}$, (py = pyridine) and $[Re(dppe)_2(bpy)]^{2+}$, (bpy = 2,2'-bipyridine).

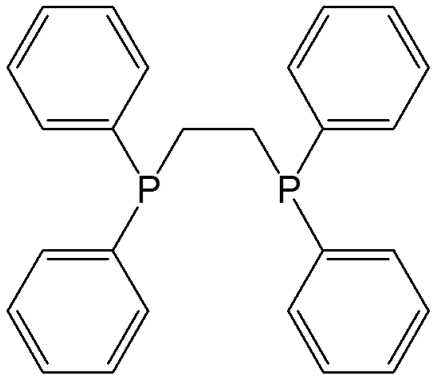

Figure 8: 1,2-Bis(diphenylphosphino)ethane (dppe)

Chapter 2: Experimental Methods

2.1 Materials

Potassium perrhenate, tetrabutylamonium bromide, ethylenebis (diphenylphosphine), pyridine, 2,2'-bipyridyl, hypophosphorous acid 50% in water solution, ammonium hexafluorophosphate were purchased from Sigma-Aldrich and used as recieved. Thallium hexafluorophosphate was purchased from Stream Chemicals, and hydrochloric acid was purchased from Fisher.

The solvents ethanol (Decon Laboratories), methanol (Fisher), propanol (OmniSolv), acetonitrile (Fisher), anhydrous ethyl ether (Fisher), dichloromethane (Fisher), benzene (Fisher), ethylene glycol dimethyl ether (Sigma-Aldrich) were used as purchased unless otherwise noted. Water was deionized to 18 MΩ by a Barnstead B-pure cartridge water purification system.

2.2 Instrumentation

^{1}H NMR spectra were measured on a Bruker 400 MHz NMR spectrometer, and mass-spectra were collected on a Bruker MicrOTOF spectrometer with electrospray ionization (ESI) equipped with an Agilent 1200 LC. Bruker Daltonics DataAnalysis version 3.4 software was used to analyze the data. Absorbance measurements were collected on a Hewllet-Packard diode array spectrophotometer (HP 8453) using a 1.0 x 1.0 cm quartz cuvette.

2.3 Synthesis and Characterization

2.3.1 Syntheis of $(Bu)_4NReO_4$

$(Bu)_4NReO_4$ was synthesized from $KReO_4$ by a published procedure.[13] Potassium perrhenate (103 mg, 0.32 mmol) was dissolved in 5 mL of hot water, and 1 mL of 0.31 M tetrabutylammonium bromide was added dropwise. A white precipitate was formed, and it was stirred for 5 minutes. The reaction mixture was cooled to room temperature and the white precipitate was filtered from the colorless solution and washed with water, 10% ethanol/diethyl ether, and diethyl ether. Yield: 103 mg (68%). ^{1}H NMR data (in d_3-MeCN): δ 0.95 (t, 3H, CH_3), 1.33 (m, 2H, CH_2), 1.59 (m, 2H, CH_2), 3.10 (t, 2H, N-CH_2).

The ^{1}H NMR spectrum of the product is shown in Figure 9, which exhibits 4 different peaks, a triplet at 0.95 ppm corresponding to the methyl group, and three peaks at 1.33, 1.59 and 3.10 corresponding to the methylenes.

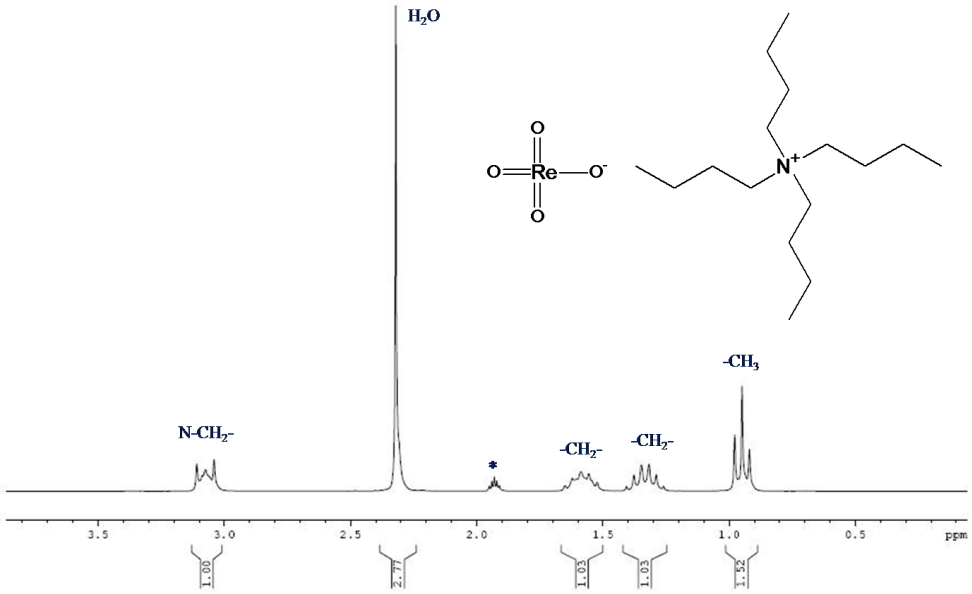

Figure 9: ^{1}H NMR spectrum of $(Bu)_4NReO_4$

Because the peaks shown in the ^{1}H NMR spectrum can also arise from the starting material, $(Bu)_4NBr$, and not from the final product, electrospray ionization mass spectrometry (ESI-MS) was used and the resulting spectrum is shown in Figure 10, which consists of two peaks. The peak at m/z 242.3 correspond to the tetrabutylammonium cation, $[Bu_4N]^+$, while the peak at m/z 735.6 correspond to the bis(tetrabutylammonium) perrhenate cation, $\{[(Bu)_4N]_2ReO_4]\}^+$. These results confirm the identity of the rhenium product, which was used as a starting material in subsequent reactions.

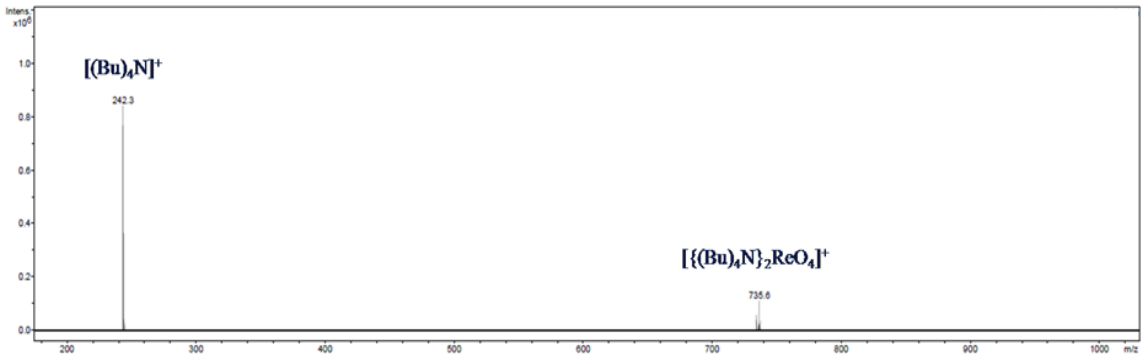

Figure 10: ESI-MS chromatogram of $(Bu)_4NReO_4$

2.3.2 Synthesis of $[Re(dppe)_2Cl_2]PF_6$

This synthesis of $[Re(dppe)_2Cl_2]PF_6$ is an adaptation from the one published by Deutsch *et. al.*[13] Tetrabutylammonium perrhenate (50 mg, 0.1015 mmol) was dissolved in 15 mL of ethanol and placed in a 50 mL round-bottom flask. A 0.35 mL portion of 12 M HCl (4.2 mmol) and 1,2-bis(diphenylphosphino)ethane (403 mg, 1.015 mmol) were added. The reaction mixture turned yellow and it was refluxed for 22 hours. After the mixture was cooled to room temperature, 5 mL of H_2O was added, with a subsequent addition of a concentrated solution of ammonium hexafluorophosphate (150 mg, 0.92 mmol). The yellow precipitate was filtered from the solution and washed with 10% ethanol/water and diethyl ether. Recrystallization from acetronitrile yielded 68% of a yellow solid.

The ^{1}H NMR of this compound showed some impurities; therefore further purification using column chromatograhy was performed, being the stationary phase alumina and acetonitrile as the solvent. The ^{1}H NMR spectrum of one of the aliquotes is shown in Figure 11. Three peaks can be observed, the one at 2.83 ppm correspond to the methylene groups of the dppe ligands and the ones at 7.26 and 7.43 ppm correspond to the phenyl groups dppe ligands.

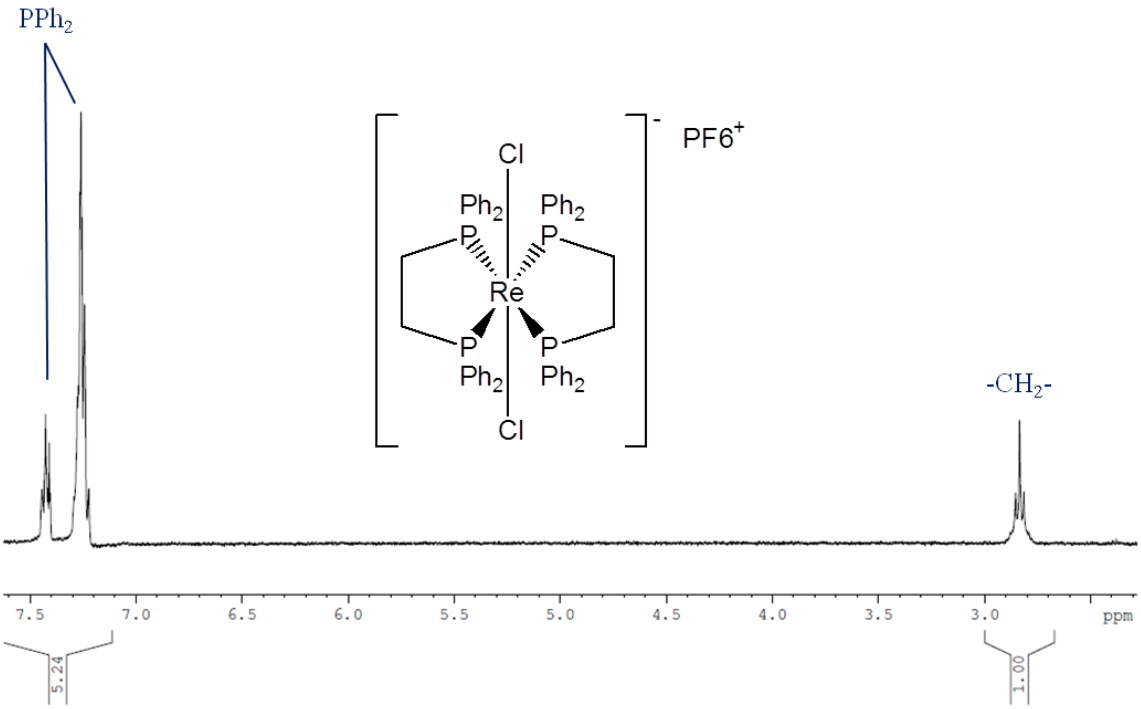

Figure 11: ^{1}H NMR spectrum of $[Re(dppe)_2Cl_2]PF_6$

Due to the many problems encountered while using this synthetic route, a different approach was taken inspired by Cotton *et. al.*[14] The starting material required for this synthesis, $[(Bu)_4N]_2[Re_2Cl_8]$, was synthesized using a published procedure.[12]

2.3.3 Synthesis of $[(Bu)_4N]_2[Re_2Cl_8]$

Sodium perrhenate (1.89 g, 6.92 mmol) and sodium chloride (2.0 g, 34.22 mmol) were heated in 40 mL of 50% aqueous hypophosphorous acid for 10 hours. Tetrabutylammonium bromide (4.0 g , 26.48 mmol) in 75 mL of 6 M hydrochloric acid was added to the dark solution and refluxed for 12 hours. The blue precipitate was filtered from the hot solution and washed with 20 mL of 6 M HCl and two 20 mL portions of ethanol. ^{1}H NMR data (in d_3-MeCN): δ 0.96 (t, 3H, CH_3), 1.35 (m, 2H, CH_2), 1.59 (m, 2H, CH_2), 3.08 (t, 2H, N-CH_2).

The ^{1}H NMR spectrum of the product is shown in Figure 12, which exhibits four different peaks, a triplet at 0.96 ppm corresponding to the terminal methyl group, and three peaks at 1.35, 1.59 and 3.08 corresponding to the methylene groups of the $(Bu)_4N^+$ counterion.

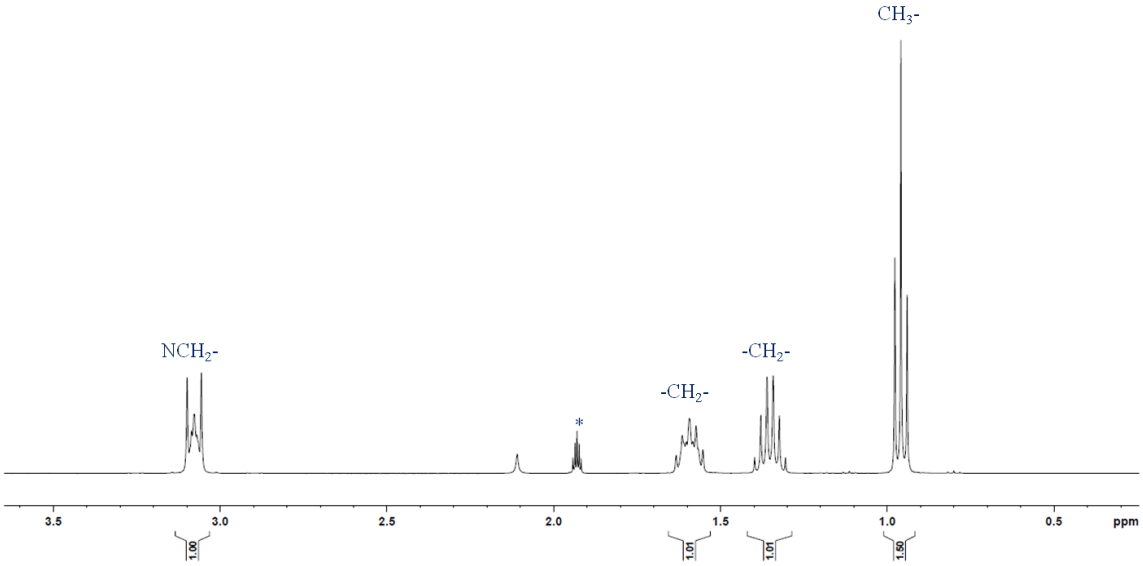

Figure 12: ^{1}H NMR spectrum of $[(Bu)_4N]_2[Re_2Cl_8]$

Because the peaks shown in the ^{1}H NMR spectrum can be attributed to the starting material, $(Bu)_4NBr$, and not from the final product, the electrospray ionization mass spectrometrum of the complex was collected and is shown in Figure 13.

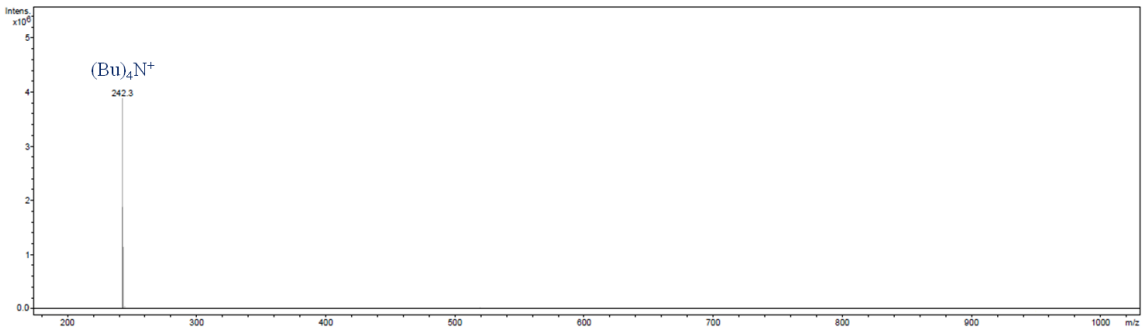

Figure 13: ESI-MS chromatogram of $[(Bu)_4N]_2[Re_2Cl_8$

The spectrum collected using positive ion mode only shows one peak at m/z 242.3 corresponding to the tetrabutylammonium cation, therefore the negative ESI-MS was used in order to determine if the desired product was successfully synthesized. It is evident from Figure 14, that there are three major peaks observed. The peak at m/z 326.8 corresponds to $Re_2Cl_8^{2-}$, the one at m/z 585.7 corresponds to $Re_2Cl_6^-$ and the peak at m/z 618.7 corresponds to $Re_2Cl_7^-$.

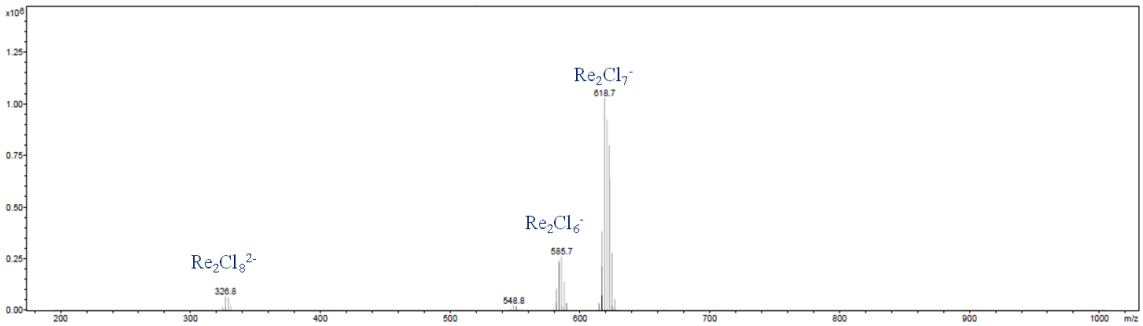

Figure 14: Negative ESI-MS chromatogram of $[(Bu)_4N]_2[Re_2Cl_8]$

2.3.4 Synthesis of $[Re(dppe)_2Cl_2]Cl$

Under a nitrogen atmosphere, a solution of $[(Bu)_4N]_2[Re_2Cl_8]$ (0.5 g, 0.438 mmol) and 1,2-bis(diphenylphosphino)ethane (1.5 g, 3.76 mmol) in 47 mL of ethanol and 3 mL of 12 M HCl was refluxed for 48 hours. The solution was cooled to room temperature and filtered to remove impurities from the yellow solution. The solid was washed with methanol until the washings were colorless. The washings and the mother liquor were concentrated to a volume of 15 mL. The orange crystals that formed were washed with methanol and diethyl ether. The ^1H NMR of this compound is shown in Figure 15.

Anal. Calcd. for $C_{52}H_{48}P_4ReCl_3$: C, 57.33; H, 4.44. Found: C, 56.35; H, 4.75

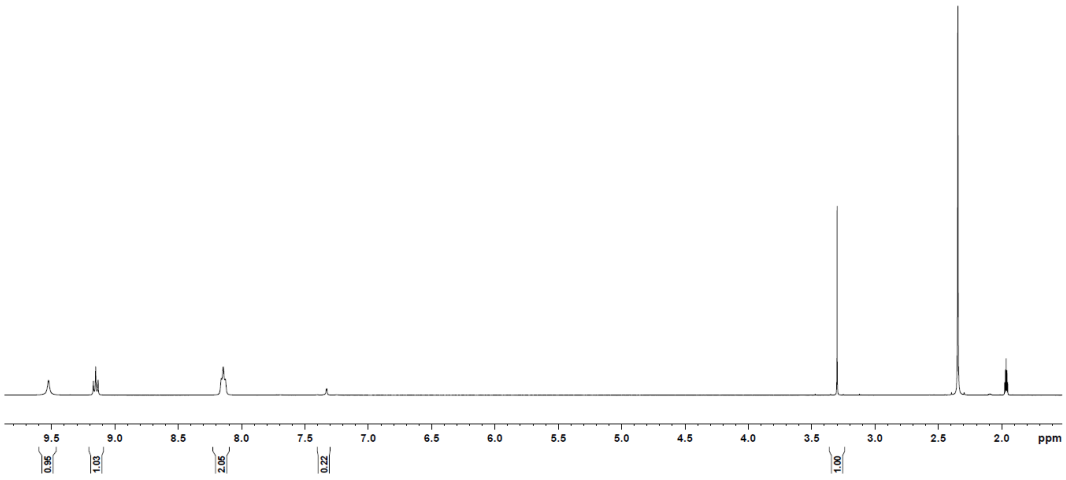

Figure 15: ^1H NMR spectrum of $[Re(dppe)_2Cl_2]Cl$

As it can be seen, the ^{1}H NMR spectra for $[Re(dppe)_2Cl_2]PF_6$ and $[Re(dppe)_2Cl_2]Cl$ are different. The only difference between these two compounds is the counter ion, therefore we could expect the ^{1}H NMR spectra to be identical. Because this is not the case, something else must had occur. In both complexes rhenium has an oxidation state of +3, meaning it has a d^4 configuration. The crystal field splitting diagram for these complexes is shown in Figure 16.

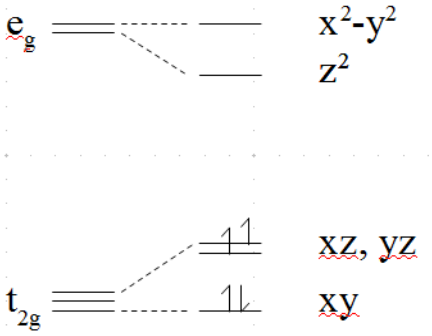

Figure 16: Crystal field splitting diagram for $[Re(dppe)_2Cl_2]^+$

As it can be seen from the figure above, the complexes are paramagnetic, therefore they won't show in the ^{1}H NMR spectra. The peaks shown are impurities from the reactions. The ESI-MS chromatogram for the $[Re(dppe)_2Cl_2]Cl$ complex was collected and is shown in Figure 17, where two major peaks can be observed. The peak at m/z 1053.1 corresponds to $[Re(dppe)_2Cl_2]^+$ and that at m/z 2143.1 corresponds to $[Re_2(dppe)_4Cl_5]^+$.

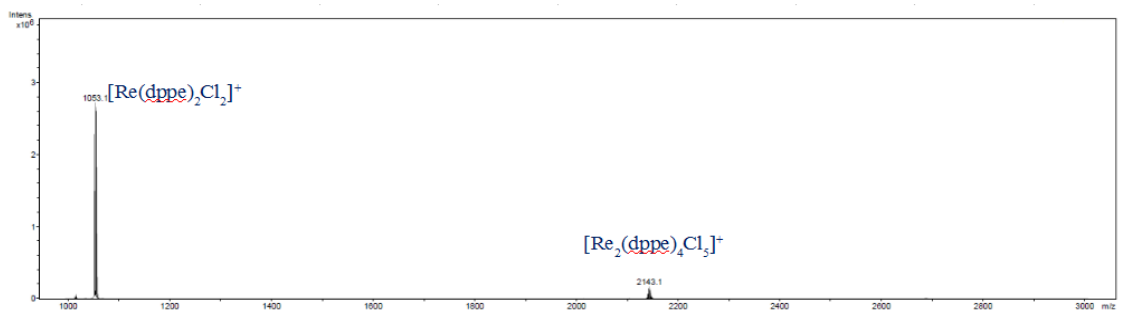

Figure 17: ESI-MS chromatogram of $[Re(dppe)_2Cl_2]Cl$

2.3.5 Synthesis of $[Re(dppe)_2O_2]ClO_4$

A solution of $[(Bu)_4N]_2[Re_2Cl_8]$ (0.30 g, 0.220 mmol) and 1,2-bis(diphenylphosphino)ethane (964 mg, 2.420 mmol) in 60 mL of methanol containing 3 mL of 60% aqueous perchloric acid was refluxed for 1 hour. The solution was allowed to cool to room temperature and the orange precipitate was filtered and washed with 10 mL of benzene and 20 mL of diethyl ether, yield 62%.

The The ESI-MS spectrum for this compound was collected and is shown in Figure 18. The only peak at m/z 1015 corresponds to $[Re(dppe)_2O_2]^+$.

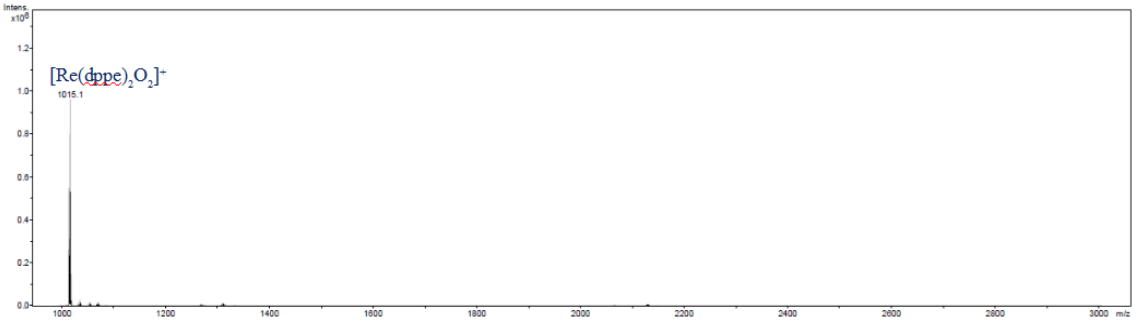

Figure 18: ESI-MS chromatogram of $[Re(dppe)_2O_2]ClO_4$

Chapter 3: Results

3.1 Spectroscopy

3.1.1 $[Re(dppe)_2Cl_2]Cl$

The combined absorption, emission and excitation spectra for the $[Re(dppe)_2Cl_2]Cl$ complex is shown in Figure 19.

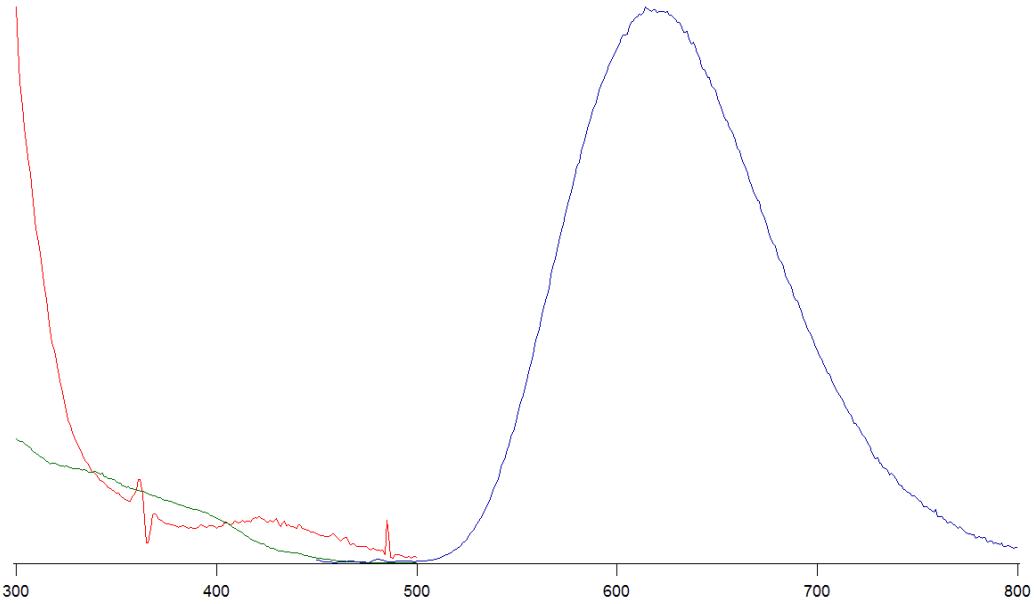

Figure 19: Combined absorption, emission and excitation spectra of $[Re(dppe)_2Cl_2]Cl$ at 77K

As it can be seen in the figure above, the absorption and excitation spectra, even though are close, are not a perfect match. It can be inferred from both the combined spectra and the previous ^{1}H NMR spectra that some impurities are present. Excitation of an acetonitrile solution of $[Re(dppe)_2Cl_2]^+$ at 420 nm yields an emission band with an emission maximum at 614 nm.

3.1.2 $[Re(dppe)_2O_2]ClO_4$

The combined absorption, emission and excitation spectra for the $[Re(dppe)_2O_2]ClO_4$ complex is shown in Figure 20.

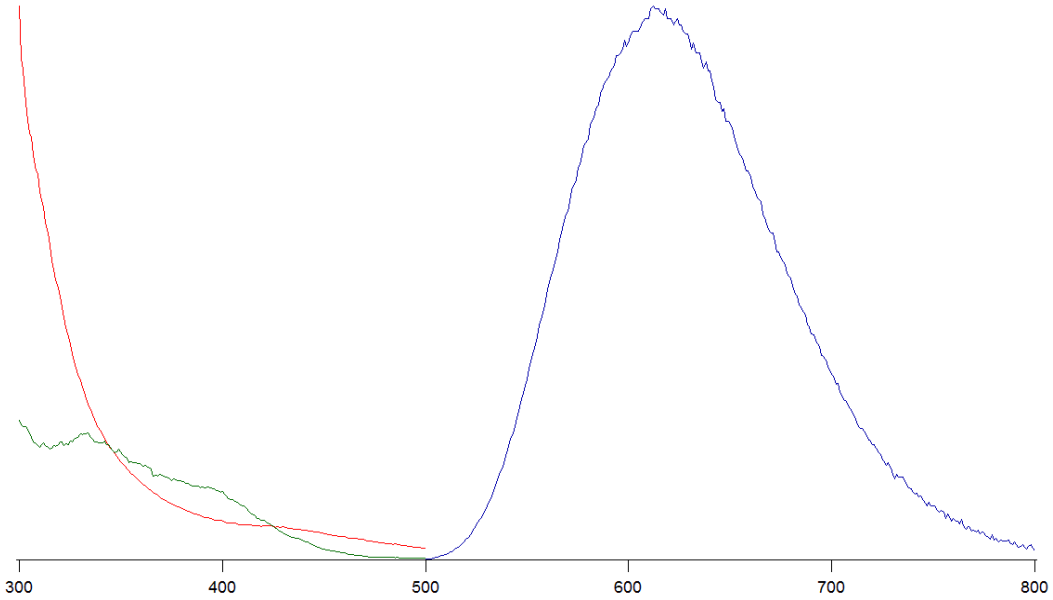

Figure 20: Combined absorption, emission and excitation spectra of $[Re(dppe)_2O_2]ClO_4$ at 77K

Excitation of an acetonitrile solution of $[Re(dppe)_2O_2]ClO_4$ at 420 nm yields an emission band with an emission maximum at 600 nm.

3.2. Electrochemistry

Cyclic voltammetry was performed for the $[Re(dppe)_2Cl_2]Cl$ complex, and the voltammogram is shown in Figure 21.

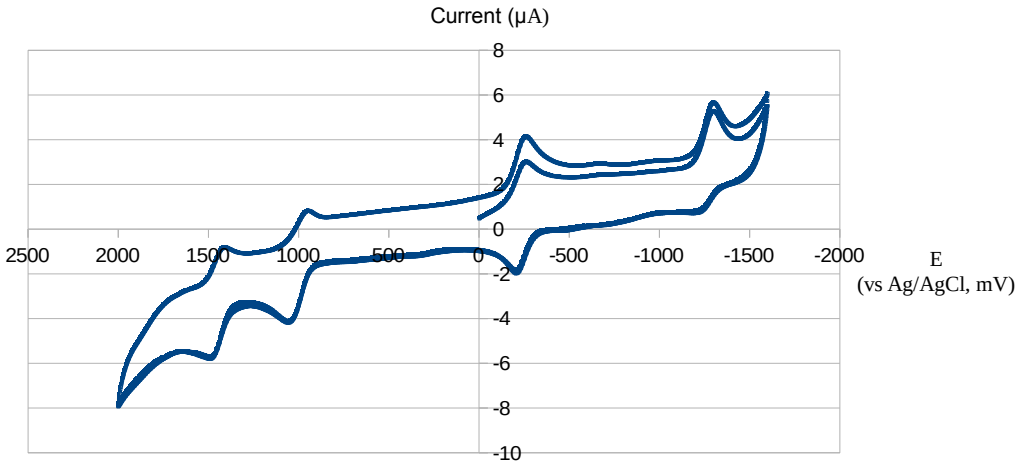

Figure 21: Cyclic Voltammogram of $[Re(dppe)_2Cl_2]Cl$ in 0.1 M $TBAPF_6$/acetonitrile at a platinum electrode

A scan initiated at 0 V in the negative direction exhibits two reduction peaks at -0.26 and -1.30 V. Upon reversal of the scan, the corresponding oxidation waves were observed at -1.21 and -0.20 V. When going to positive potentials, two oxidation peaks can be found at 1.06 and 1.50 V, with the corresponding reduction waves at 1.41 and 0.95 V. The peak to peak separation for these redox couples are 60, 90, 112 and 92 mV respectively. According to the Nerst equation this value should be 59 mV for a one electron reversible couple. On the basis of that, we can say that the first redox couple with an E^o of -0.03 V vs SHE, was found to be reversible, while the other three are not. If this compound was part of a DSSC it will first get reduced upon receiving electrons coming from the circuit, and later will get oxidized, reducing the triiodide to iodide. The latter is due to the fact that the redox potential for I_2/I^- is 0.54 V vs SHE. Based on the reversibility of the redox reaction and the reduction potential being lower than the potential for iodine/iodide, it can be asumed that the $[Re(dppe)_2Cl_2]Cl$ complex will be suitable as a dye for the photocathode in a tandem DSSC.

Chapter 4: Conclusions

The compounds $[Re(dppe)_2Cl_2]Cl$ and $[Re(dppe)_2O_2]ClO_4$ were sinthesized and characterized by ^1H NMR and ESI-MS. Both compouds exhibit significant absorbance at around 600 nm, something that is characteristic for phosphine rhenium complexes.

The cyclic voltammogram performed on the $[Re(dppe)_2Cl_2]Cl$ complex shows that the first reduction with a potential of -0.03 V vs SHE is reversible. This potential, being lower than the reduction potential for iodine/iodide, suggests that this compound would be suitable as a dye fot the photo cathode in a tandem dye sensitized solar cell.

Further work is still needed in order to determine how the overall efficiency of a tandem DSSC would be affected when using this compound as a dye for the photo cathode.

References

[1] Grätzel, M. *J. Photochem. Photobiol., C.* **2003**, 4, 145-153.

[2] Chapin, D. M.; Fuller, C. S.; Pearson, G. L. *J. Appl. Phys.* **1954**, 25, 676-677.

[3] Grant, C. D.; Schwartzberg, A. M.; Smestad, G.P.; Kowalik, J.; Tolbert, L. M.; Zhang, J. Z., *J. Electroanal. Chem.* **2002**, 522, 40-48.

[4] O'Regan, B.; Grätzel, M. *Nature* **1991**, 353, 737-740.

[5] Yella, A.; Lee, H.; Tsao, H.; Yi, C.; Chandiran, A.; Nazeerudin, K.; Diau, E.; Yeh, C.; Zakeeruddin, S.; Grätzel, M. *Science*, **2011**, 334, 629-634.

[6] Li, B.; Wang, L.; Kang, B.; Wang, P.; Qiu, Y. *Sol. Energ. Mat. Sol. C.*, **2006**, 90, 549-573.

[7] Hamann, T.W.; Jensen, R.A.; Martinson, A.B.; Van Ryswyk, H.; Hupp, J.T. *Energy Environ. Sci.* **2008**, 1, 66-78.

[8] Pagliaro, M., Palmisano, G., Ciriminna, R. and Loddo, V. Energy Environ. Sci., **2009**, **2**, 838-844.

[9] Clifford, J.N.; Palomares, E.; Nazeeruddin K.; Grätzel M.; Durrant J. *J. Phys. Chem.*, **2007**, 111, 6561-6567.

[10] He, J.; Lindström, H.; Hagfeldt, A.; Lindquist, S.-E. *Sol. Energy Matter. Sol. Cells*, **2000**, 62, 265-273.

[11] Gibson, E.; Smeigh, A.; Pleux, L.; Fortage, J.; Boschloo, G.; Blart, E.; Pellegrin, Y.; Odobel, F.; Hagfeldt, H.; Hamamarström, L. *Angew Chem.* **2009**, 121, 4466-4469.

[12] Del Negro, A.S.; Seliskar, C.J.; Heineman, W.R.; Hightower, S.E.; Bryan, S.A.; Sullivan, B.P. *J. Am. Chem. Soc.* **2006**, 128, 16494-16495.

[13] Vanderheyden, J.; Heeg, M.J.; Deutsch E. *Inorg. Chem.*, **1985**, 24, 1666-1673.

[14] Cotton, F.A.; Curtis, N.F.; Robinson, W.R. *Inorg. Chem.*, **1965**, 4, 1696-1700.